



## Synthesis of ZnO NWs via Thermal Evaporation Technique

<sup>1</sup>Wafaa Khalid Khalef\*, <sup>2</sup>Abdul-Qader Dawood Faisal, <sup>1</sup>Ali A. Aljubouri

<sup>1</sup>Department of Applied Science, University of Technology, Iraq

<sup>2</sup>Ibn Khaldun Private University College, Iraq

### Article information

#### Article history:

Received: November, 20, 2023

Accepted: February, 09, 2024

Available online: October, 20, 2024

#### Keywords:

ZnO nanofilm,

ZnO nanowires,

Zn metal evaporation

#### \*Corresponding Author:

Wafaa Khalid Khalef

[drwafaa1980@gmail.com](mailto:drwafaa1980@gmail.com)

#### DOI:

<https://doi.org/10.53523/ijoirVol11I2ID421>

This article is licensed under:

[Creative Commons Attribution 4.0 International License](https://creativecommons.org/licenses/by/4.0/).

### Abstract

Zinc oxide nanowires ZnONWs were successfully synthesized on glass slides. The synthesis was conducted firstly by the deposition of 12  $\mu\text{m}$  a thin film of Zn metal by thermal evaporation. Secondly, the coated film was annealed at a temperature of 600  $^{\circ}\text{C}$  in air for four hours to grow the ZnO nanowires. It has been observed that the produced nanowires were grown in a vertical orientation and having a high density, very long, and a minimal aspect ratio. The crystal structure and morphology of ZnO nanowires were investigated with X-ray diffraction (XRD) and scanning electron microscopy (SEM). The UV-visible spectrophotometer was also used to calculate the optical parameters from the absorption spectrum and show a band gap energy around 3.25 eV. The crystal structure of the material was revealed to be polycrystalline with a preferred orientation in the direction of [101]. Small average crystallite size was calculated about 17nm. The wires can be measured to have a length of around 10  $\mu\text{m}$  with diameters ranging from 50 to 100 nm. This could be used for gas sensor applications. In addition, this ZnONWs structure has a maximum transmittance (100%) which can be a good candidate for many optoelectronic applications.

### 1. Introduction

In this introduction, we will discuss the fundamentals of the synthesis of ZnO nanowires using the thermal evaporation method, as well as the benefits of this approach and the difficulties that it presents. It will also cover some of the significant developments and possible uses of ZnO nanowires that were manufactured using this method, highlighting the significance of this method in the field of nanomaterials and nanotechnology. In the field of nanomaterials, Zinc Oxide (ZnO) nanowires have attracted a lot of attention due to the distinctive structural [1], electrical [2], and optical features [3] that they possess. These nanowires have the potential to be useful in a wide variety of applications, such as photocatalysts, energy harvesting devices, optoelectronic devices, and sensors, among others [4-7]. The thermal evaporation technique is one of the many methods that can be used to synthesize ZnO nanowires [8,9], and it stands out as a method that is both versatile and effective. The formation of ZnO nanowires on a suitable substrate can be accomplished using a process known as thermal evaporation, which involves the controlled vaporization of a Zn source material (usually metallic zinc powder) under regulated conditions. Using this method, one may generate high-quality ZnO nanowires that have well-defined morphologies, tunable diameters, and crystalline structures. This is only one of the many benefits that this technology provides. In addition to this, it offers a method for the creation of nanowires that is both affordable and scalable. Researchers can modify the features of ZnO nanowires to match the requirements of a

particular application by improving these factors. Additionally, the thermal evaporation process enables the development of vertically aligned ZnO nanowire arrays, which are particularly suitable for sensor and optoelectronic applications [ 3]. The process of exposing thin films of metallic Zn to heat oxidation is yet another method that is frequently utilized in the synthesis of ZnO nanowires. There is a mention of the authors Wafaa et al. in reference number 3, as well as in publications number 8 and 9. B. D. Yao et al [10] Mass production of ZnO nanowires, nanoribbons, and needle-like rods has been achieved by a simple method of thermal evaporation of ZnO powders mixed with graphite. A. Chrissanthopoulos et al [11] reported the formation of ZnO/carbon nanotubes heterostructures achieved using a thermal evaporation method. Scanning electron microscopy revealed that the main building block of the observed morphologies was the nanorod whose self-assembling resulted in various structures such as polypods and nano-hedgehogs, depending on various factors as well as the location of the ZnO–CNT junction. Using thermal oxidation of metallic zinc, researchers were able to produce improved ZnO films and document the process. The thermal oxidation of metallic zinc films in an atmosphere with a high concentration of oxygen can be used as a method for the production of zinc oxide films that have a high level of both purity and quality. Furthermore, this methodology was employed in the aforementioned study, which presents a straightforward, cost-effective, non-catalytic approach for fabricating ZnO nanowires. Zinc oxide (ZnO) nanowires were synthesized on glass substrates using the process of thermal oxidation of thin metallic zinc films in an air environment, at a temperature of 600°C for 4 hours. This study presents the process of synthesizing ZnO nanowires through the thermal oxidation of a zinc layer.

## 2. Experimental Procedure

The glass slides were used for Zinc metal film support. Firstly, they were washed with water and subjected to ultrasonic cleaning using acetone and alcohol for approximately 15 minutes each. Then rinsed with deionized water. Zinc metal powder of high purity (commercial grade) was loaded into the Physical Vapor Deposition (PVD) chamber. Zinc oxide (ZnO) nanowires were fabricated on glass slides through the oxidation process of zinc (Zn) metal films using physical vapor deposition (PVD) as shown in Figure (1). The distance between the substrate and the source during the process was set at 10cm apart. The laser method was used to measure the thickness of the deposited film. The films with a thickness of around 30µm was measured. The thermal oxidation process of the deposited substrates (Zn/glass) was conducted as a distinct experiment. The substrates were placed onto an alumina boat and subsequently inserted into the center of a one-meter quartz tube within an electric tube furnace. The oxidation studies were conducted for 4 hours in an ambient air environment at a temperature of 600°C. The heating rate was approximately 25 degrees Celsius per minute. After the oxidation process, the furnace was deactivated and allowed to cool down naturally. The materials were then analyzed using X-ray diffraction (XRD), scanning electron microscopy (SEM), and UV-visible spectrophotometry.

The film was analyzed using an X-ray diffraction (XRD-Shimadzu 6000/Japan) diffractometer with Cu K $\alpha$  radiation ( $\lambda=0.15406$  nm) in the 2 theta range of 30° to 80°. The form and size of the ZnO nanostructures in the product were determined using high-resolution scanning electron microscopy (SEM) with a Tescan Vega II-Cheek instrument. The X-ray diffraction (XRD) technique with CuK $\alpha$  radiation ( $\lambda = 0.15406$  nm) was used to analyze the crystal structures of the samples. Scanning electron microscopy (SEM/ Tescan Vega II- Cheek) was used to analyze the surface morphologies and components of the oxidized Zn sheets. The UV-visible spectrophotometer was used to test the optical transmittance.



Figure (1): Vacuum Evaporative (PVD) System.

### 3. Results and Discussion

#### 3.1. XRD Analysis

An investigation of the crystal structure of ZnO NWs was carried out. The XRD patterns of the fabricated film by thermal oxidation of the Zn metal layer at temperatures of 600 degrees Celsius is displayed in Figure (2). The reflection planes (100), (002), (101), (102), (110), (103), and (112) are comparable to the peaks that occur at 32.2°, 34°, 36°, 47°, 56°, 63°, 68°, and 77°, respectively. The ZnO (101) is the dominant peak that can be seen in Figure at  $2\theta=36.564^\circ$  which represents the preferred orientation of the structure. The diffraction peaks are easily assignable to a ZnO structure that does not have a preferred orientation, and they are in good accord with the standard data of JCPDS # 36-1451. The crystallite size was calculated using the Sherrer equation [10-12].

$$D = 0.9\lambda/\beta \cos\theta \quad (1)$$

The constant k is considered to have a value of 0.94. The utilized X-ray wavelength, denoted by  $\lambda$ , is supposed to be 1.54 Å.  $\theta$  represents Bragg's angle, and  $\beta$  represents the entire width at half maximum of the X-ray diffraction patterns. The dimensions of the crystallites are presented in Table (1).

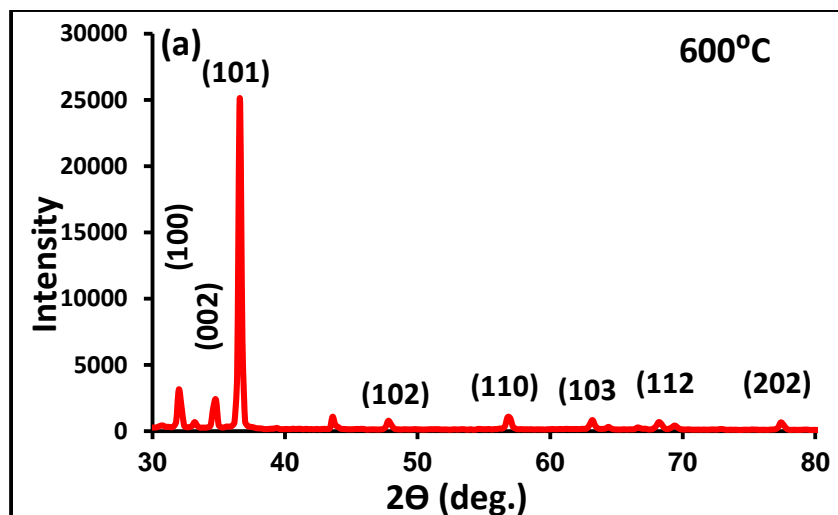


Figure (2): X-ray diffraction (XRD) of ZnO film oxidized at 600°C.

**Table (1):** ZnO/ NWs parameters.

Sample	The temperature of Oxidation (°C)	2-theta ( $2\theta^\circ$ )	Fill width of half maximum (FWHM)	Crystallite size (nm)
ZnO NWs	600	36.5645	0.4869	17.9

### 3.2. SEM Analysis

Figure (3) displays scanning electron microscopy (SEM) images of a ZnO/glass film formed by oxidizing it at a temperature of 600°C for 4 hours in air. The presented images were taken at various magnifications. Figure (3a) displays a vast distribution of ZnO nanowires with the maximum density and length which was covered a significant portion of the substrate. The film of the nanowires exhibit several wrinkles. The wires can be measured to have a length of around 10  $\mu\text{m}$  with diameters ranging from 50 to 100 nm. The medium and high SEM magnification images in Figure (3b) and c displayed a wire arrangements.

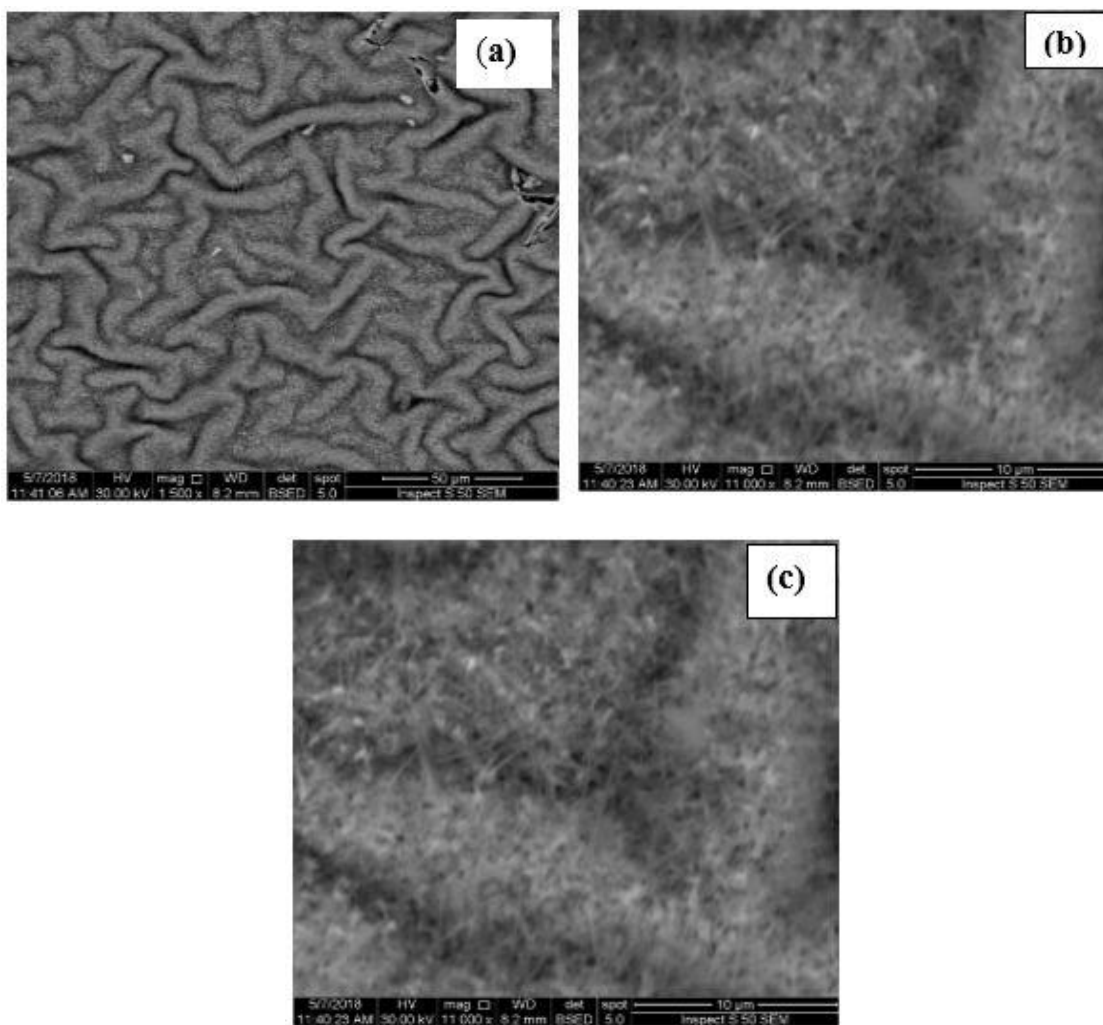


**Figure (3):** different magnifications of SEM images of ZnO deposited on a glass substrate and oxidized at 600°C.

EDX was used to analyze the bulk element compositions of the ZnO NWs, and Figure (4) displays the spectrum obtained from this analysis. The high ratios of zinc and oxygen elements found in ZnO nanostructures lend credence to the theory that no additional metal components are utilized in the process of accelerating the formation of ZnO nanostructures.



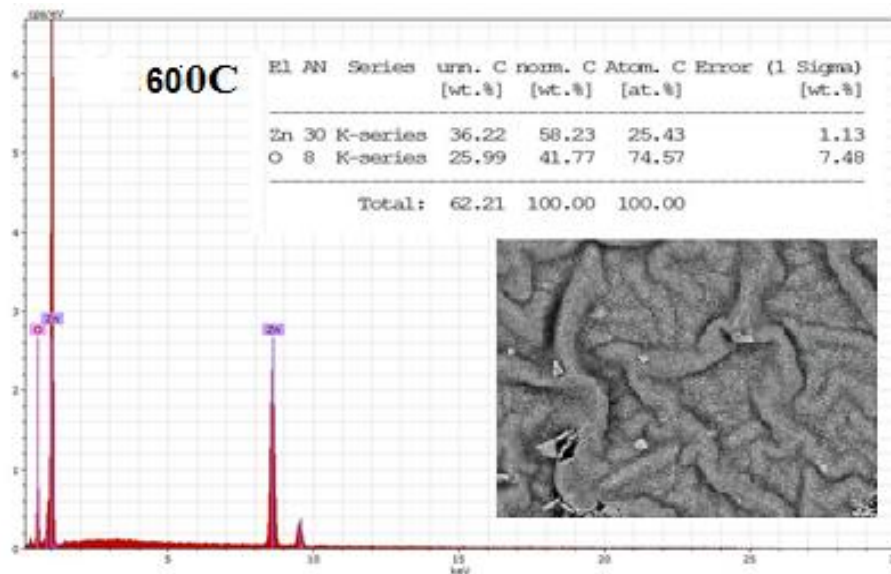


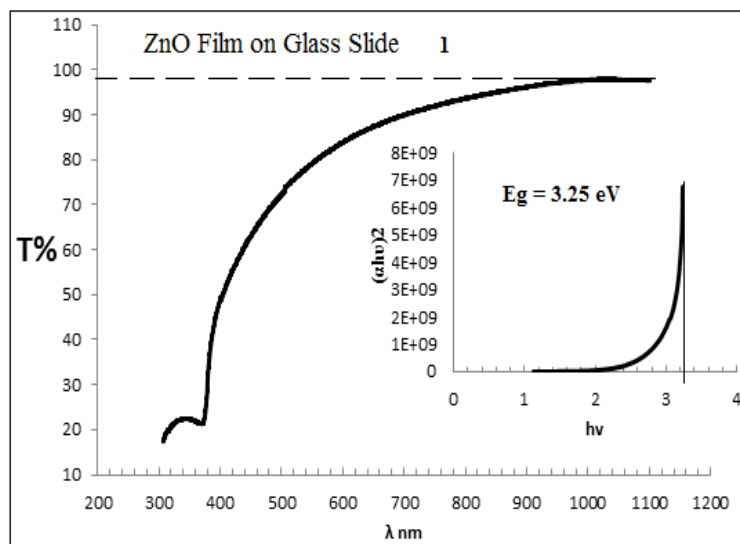
Figure ( 4): DES for ZnO NWs on the substrate of a glass and oxidized at 600C for 4 hours.

### 3.3. Optical Properties

The transmittance spectra of ZnO films in the wavelength range of 200–1200 nm are shown in Figure (5). The average transmittance of ZnO film is about 95% in the visible region (400–700 nm). This is a duo to ZnO the transparent conductive oxide (TCO) material [11 ]. The absorption coefficient  $\alpha$  is correlated to the optical band gap by the following equation [14,13].

$$(\alpha h\nu)^2 = A(h\nu - E_g) \quad (2)$$

In this equation,  $h$  represents Planck's constant,  $\nu$  represents the incident photon frequency,  $A$  represents a constant, and  $E_g$  represents the optical band gap. Tuac's graphic provides the formula for calculating the optical band gap of ZnO films by extrapolating the linear portion of the  $(h\nu)^2$  curve toward the energy  $h$  axis at  $(h\nu)^2 = 0$ . ZnO film band gap was measured. ZnO films have a predicted band gap of roughly 3.25 eV (Zn film oxidation temperature of 600°C for 4h, as depicted in the inset of Figure. This is due to the decrease in particle size of ZnO which could be attributed to the quantum confinement [14-16]. The  $E_g$  values are in good agreement with other workers [ 17].



Figure( 5): Optical transmittance of ZnO film on quartz slides (Zn film oxidation temperature of 600°C for 4h). The inset shows the optical band gap calculated by the  $(\alpha h\nu)^2$ -energy of the transmittance curve.

#### 4. Conclusions

In conclusion, Zn metal powder can be easily evaporated used Physical Vapor deposition to grow ZnO NWs. ZnO nanowires were successfully synthesized via the physical vapor deposition method (PVD). X-ray diffraction shows, a polycrystalline wire structure with a preferred orientation (101). The SEM results show a Long, small, high-density, and well-aligned ZnO nanowires were obtained with different diameters and lengths of the wires in nanometers. The optical properties of the absorption spectrum with ZnO energy band gap of about 3.25 eV. This also confirms the formation of the well oriented of ZnO crystal structure.

#### Acknowledgment

We would like to offer special thanks to the head of the Department of Applied Science Prof. Dr. Raid A. Ismail, and to the senior of the Applied Science Research Unit Prof. Dr. Evan Tariq for their grateful support and resources provided which led to the successful completion of the project.

**Conflict of Interest:** The authors declare that there are no conflicts of interest associated with this research project. We have no financial or personal relationships that could potentially bias our work or influence the interpretation of the results.

#### References

- [1] A. A. Aljubouri, A. D. Faisal, and W. K. Khalef, "Fabrication of temperature sensor based on copper oxide nanowires grown on titanium coated glass substrate," *Materials Science-Poland*, vol. 36, no. 3, pp. 460–468, Sep. 2018, doi: 10.2478/msp-2018-0051.
- [2] K. A. Esvar *et al.*, "Hydrothermal growth of flower-like ZnO nanostructures on porous silicon substrate," *Journal of Molecular Structure*, vol. 1074, pp. 140–143, Sep. 2014, doi: 10.1016/j.molstruc.2014.05.067.
- [3] W. K. Khalef, A. A. Aljubouri, and A. D. Faisal, "Photodetector fabrication based ZnO nanostructure on a silicon substrate," *Optical and Quantum Electronics*, vol. 52, no. 7, Jun. 2020, doi: 10.1007/s11082-020-02445-y.
- [4] A. Thamer, A. Faisal, A. Abed, and W. Khalef, "Synthesis of gold-coated branched ZnO nanorods for gas sensor fabrication," *Journal of Nanoparticle Research*, vol. 22, no. 4, Mar. 2020, doi: 10.1007/s11051-020-04783-0.
- [5] Z. L. Wang, "Zinc oxide nanostructures: growth, properties and applications," *Journal of Physics: Condensed Matter*, vol. 16, no. 25, pp. R829–R858, Jun. 2004, doi: 10.1088/0953-8984/16/25/r01.
- [6] J. Ghosh, R. Ghosh, and P. K. Giri, "Tuning the visible photoluminescence in Al-doped ZnO thin film and its application in label-free glucose detection," *Sensors and Actuators B: Chemical*, vol. 254, pp. 681–689, Jan. 2018, doi: 10.1016/j.snb.2017.07.110.
- [7] V. Consonni, J. Briscoe, E. Kärber, X. Li, and T. Cossuet, "ZnO nanowires for solar cells: a comprehensive review," *Nanotechnology*, vol. 30, no. 36, p. 362001, Jun. 2019, doi: 10.1088/1361-6528/ab1f2e.
- [8] I. Abdulkarim Ali, "Characterization of Zinc oxide Nanostructures prepared by hydrothermal method with Antibacterial property," *Iraqi Journal of Physics*, vol. 17, no. 42, pp. 108–124, Aug. 2019, doi: 10.30723/ijp.v17i42.448.
- [9] W. K. Khalef, A. A. Aljubour, and A. D. Faisal, "Glucose biosensor electrode fabrication based on CuO /ZnO nanostructures," *Journal of Physics: Conference Series*, vol. 1795, no. 1, p. 012038, Mar. 2021, doi: 10.1088/1742-6596/1795/1/012038.
- [10] B. D. Yao, Y. F. Chan, and N. Wang, "Formation of ZnO nanostructures by a simple way of thermal evaporation," *Applied Physics Letters*, vol. 81, no. 4, pp. 757–759, Jul. 2002, doi: 10.1063/1.1495878.
- [11] A. Chrissanthopoulos, S. Baskoutas, N. Bouropoulos, V. Dracopoulos, D. Tasis, and S. N. Yannopoulos, "Novel ZnO nanostructures grown on carbon nanotubes by thermal evaporation," *Thin Solid Films*, vol. 515, no. 24, pp. 8524–8528, Oct. 2007, doi: 10.1016/j.tsf.2007.03.146.
- [12] F. C. Eze, "Optical characterization of thin film cadmium oxide prepared by a modified reactive thermal evaporation process," *Global Journal of Pure and Applied Sciences*, vol. 9, no. 4, Apr. 2004, doi: 10.4314/gjpas.v9i4.16066.
- [13] W. K. Khalef, E. K. Hamza, and A. A. Salman, "Morphology, Optical and Electrical Properties of Tin Oxide Thin Films Prepared by Spray Pyrolysis Method," *Engineering and Technology Journal*, vol. 33, no. 3B, pp. 539–546, Mar. 2015, doi: 10.30684/etj.33.3b.13.

- [14] S. Siva Kumar, V. Ranga Rao, and G. Nageswara Rao, "Effect of morphology, crystallite size and optical band gap on photocatalytic activity of ZnO nanostructures for decolorization of R6G," *Materials Today: Proceedings*, vol. 62, pp. 5494–5502, 2022, doi: 10.1016/j.matpr.2022.04.220.
- [15] K. S. Park, J. Baek, Y.-E. Koo Lee, and M. M. Sung, "Fabrication of a wafer-scale uniform array of single-crystal organic nanowire complementary inverters by nanotransfer printing," *Nano Convergence*, vol. 2, no. 1, Feb. 2015, doi: 10.1186/s40580-014-0033-3.
- [16] P. Yang *et al.*, "Controlled Growth of ZnO Nanowires and Their Optical Properties," *Advanced Functional Materials*, vol. 12, no. 5, p. 323, May 2002, [Online]. Available: [http://dx.doi.org/10.1002/1616-3028\(20020517\)12:5<323::aid-adfm323>3.0.co;2-g](http://dx.doi.org/10.1002/1616-3028(20020517)12:5<323::aid-adfm323>3.0.co;2-g).
- [17] J. Yang, Y. Wang, J. Kong, M. Yu, and H. Jin, "Synthesis of Mg-doped hierarchical ZnO nanostructures via hydrothermal method and their optical properties," *Journal of Alloys and Compounds*, vol. 657, pp. 261–267, Feb. 2016, doi: 10.1016/j.jallcom.2015.10.117.